International Journal of Mass Spectrometry and Ion Physics, 41 (1981) 17—29
Elsevier Scientific Publishing Company, Amsterdam — Printed in The Netherlands

FISSION FRAGMENT IONIZATION MASS SPECTROMETRY: METASTABLE DECOMPOSITIONS

B.T. CHAIT and F.H. FIELD

The Rockefeller University, New York, NY 10021 (U.S.A.)

(Received 26 May 1981)

ABSTRACT

Distorted peak shapes observed in ^{252}Cf fission fragment ionization mass spectrometry using time-of-flight mass spectrometers are shown to result from delayed dissociations of initial ions. Decompositions occurring in the ion acceleration region produce tails on parent or fragment ion peaks, and decompositions occurring with the conversion of internal to kinetic energy in the field-free ion drift region produce broadenings of the parent ion peaks. In this work the various processes have been investigated by the application of appropriate retarding potentials. Examples of the various decomposition processes are given. The magnitudes of the internal energies converted are given for several processes. The application of suitable retarding potentials can be used to suppress decomposition products and enhance resolution and to determine the identities of the decomposition processes.

INTRODUCTION

Californium-252 fission fragment ionization mass spectrometry is a method which produces significant quasi-molecular (QM) ion yields for large, involatile, and fragile molecules of biological interest [1—3]. A feature of the spectra obtained using this technique is the broad and complex peak shapes which are frequently observed. For example, the $(M + Na)^+$ QM ion peak at m/z 3487 from the 31-residue polypeptide β-endorphin was observed [4] to have a full width at 1/10 maximum (FWTM) of 350 daltons and a full width at half-maximum (FWHM) of 78 daltons. The $(M + Na)^+$ peak at m/z 4741 from a protected decanucleotide was observed [5] to have an FWTM of some 600 daltons and an FWHM of 167 daltons. Macfarlane and co-workers [2,6] found that the QM peak from chlorophyll *a* at m/z 893 had an FWTM of ~30 daltons and an FWHM of ~9 daltons. Experiments in this laboratory confirm this peak breadth. Other examples of somewhat lighter compounds which exhibit broad peak shapes are given in refs. 1—5.

In the present study the source of this peak broadening has been investigated for several compounds, including the tripeptide alanylalanylalanine (AlaAlaAla), guanosine, 5′-adenosine monophosphate (5′-AMP) erythromy-

0020-7381/81/0000—0000/$02.50

cin, and chlorophyll *a*. A major cause of the broadening is the metastable decomposition of ions in flight, with release of kinetic energy. We have elucidated the primary metastable decay reactions observed for AlaAlaAla and guanosine, and have determined the amount of kinetic energy released during fragmentation. Finally it is demonstrated how the peak broadening effect may be eliminated or reduced so that higher resolutions may be obtained.

EXPERIMENTAL

A complete description of the apparatus is given elsewhere [3]. A schematic representation of the instrumental configuration employed in the present investigation is shown in Fig. 1. The compounds investigated were electrosprayed onto thin (6.3 μm) aluminized polyester film (Alexander Vacuum Research, Inc., Greenfield, MA) to a thickness of 10 $\mu g\ cm^{-2}$. All of the compounds used in this study with the exception of chlorophyll *a* were obtained from the Sigma Chemical Co. (Saint Louis, MO). The chlorophyll *a* sample was obtained from the laboratory of Prof. D. Mauzerall at the Rockefeller University. A ^{252}Cf source with a strength of 8 μCi was used, giving a flux of 1200 fission fragments per second through the sample foil of diameter 1.2 cm.

Acceleration potentials of up to ±10 kV with respect to the grounded flight tube were applied to the sample foil. An electrostatic particle guide [7,3] was employed to enhance the transport efficiency of ions down the 3-m flight tube. Potentials of ±12 V applied to the central wire resulted in a 25-fold increase in the transport efficiency of ions without significantly degrading the resolution of the instrument, which is ~2000 (FWHM) at mass 250.

Two lines of investigation were pursued to test the hypothesis that the peak broadening is caused by the metastable decomposition of ions in flight. In one, the residence time of ions in the acceleration zone between the sample foil and grid 1 (see Fig. 1) was varied by applying voltages of up to ±9 kV to grid 1. Grid 2 was kept grounded at all times. The grids were constructed from 90%-transmission electroformed nickel mesh (Buckbee—Mears Co., St. Paul, MN). The distance between the sample foil and grid 1 was 4.5 mm and that between grids 1 and 2 was 5.0 mm. In the other line of investigation,

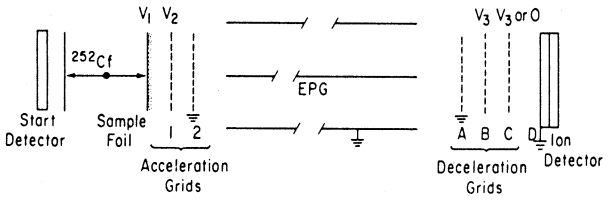

Fig. 1. Schematic representation of fission fragment ionization TOF mass spectrometer.

metastable fragments were separated from their parent ions on the basis of their different kinetic energies. This was accomplished by using a set of three deceleration grids placed directly in front of the ion detector at the end of the flight tube (Fig. 1). Grid A was grounded, while decelerating potentials of up to ±9 kV could be applied to either or both of grids B and C. The distance between grids A and B was 8.7 mm, between grids B and C, 11.9 mm, and between grid C and the detector face D, 6.3 mm. The ion detector was a chevron microchannel plate array 1.8 cm in diameter (Varian LSE, Palo Alto, CA) operated with the side facing the oncoming ions grounded.

The pressure was typically $3—10 \times 10^{-8}$ torr for the measurements reported here.

METASTABLE ION DECOMPOSITIONS IN THE TIME-OF-FLIGHT MASS SPECTROMETER

Several investigators [8—13] have studied metastable reactions in modified time-of-flight mass spectrometers. Those aspects which are relevant to the present study are reviewed here.

Consider the reaction

$$m_i^+ \rightarrow m_f^+ + m_0 \tag{1}$$

(m_i^+ = parent (initial) ion; m_f^+ = fragment ion; m_0 = neutral fragment) occurring in the field-free flight tube after m_i^+ has been fully accelerated to an energy qV_1. If no internal energy is released in the form of translational energy during fragmentation, the flight times of the undissociated parent ions m_i^+ and the metastable fragments m_f^+ and m_0 will all be the same, since their velocities are not perturbed. These components will thus appear as a single peak at time t_1 in the velocity-measuring time-of-flight instrument. However, they possess different kinetic energies given by:

$$\begin{aligned} E_i &= qV_1 \\ E_f &= (m_f/m_i)\, qV_1 \\ E_0 &= (m_0/m_i)\, qV_1 \end{aligned} \tag{2}$$

Thus the single peak may be separated into its three components by the application of a retarding potential V_3 to the central grids (B and C) of the deceleration assembly shown in Fig. 1. In the field-free region between grids B and C the kinetic energies of the three components are:

$$\begin{aligned} E_i' &= q(V_1 - V_3) \quad \text{for } V_3 \leqslant V_1 \\ E_f' &= (m_f/m_i)\, qV_1 - qV_3 \quad \text{for } V_3 \leqslant (m_f/m_i)\, V_1 \\ E_0' &= (m_0/m_i)\, qV_1 \end{aligned} \tag{3}$$

The neutral fragment m_0 is obviously unaffected by the deceleration potential and will thus appear at the same flight time t_1 as the composite peak ob-

tained in the absence of retardation. A second peak corresponding to the parent ion m_i^+ will appear which is delayed with respect to the neutral fragment peak because the ion has a reduced energy (velocity) for a fraction of the flight path. The metastable fragment ions m_f^+ will undergo an even greater shift to longer flight times because of the greater relative reduction in their energy (and thus velocity). Equations describing these time shifts are given in ref. 8.

If the potential V_3 applied to the retarding grids is greater than or equal to $(m_f/m_i)\ V_1$, the metastable fragment m_f^+ will be repelled and will not reach the detector. Thus the value of the retarding potential V_3 for which the metastable fragment peak disappears can be used to deduce the mass of the metastable fragment ion. Alternatively, a repelling potential may be applied to prevent m_f^+ metastable fragment ions from contributing to the spectrum, for the purpose of resolution enhancement (see later).

Beynon and his co-workers [14,15] have considered the effect of the release of internal energy as kinetic energy during the metastable fragmentation of ions. They obtained for T, the internal energy of m_i^+ that is converted into translation energy in the fragmentation, the expression

$$T = (m_i^2/16 m_f m_0)(\Delta E)^2/E \qquad (4)$$

where ΔE is the energy spread of the metastable fragments m_f^+, and $E = qV_1$. The quantity ΔE may be determined either from the width of the metastable peak or from the range of repeller voltages near threshold over which the metastable fragment peak disappears, and by using eqn. (4) this provides a measure of T.

Consider now the dissociation of ions in the acceleration region between the sample foil and the first grid, i.e. grid 1 in Fig. 1. Two limiting cases are straightforward to visualize, i.e., (*1*) break-up occurring close to the sample foil, and (*2*) break-up occurring close to the first grid:

Case 1. If break-up occurs on or very close to the sample foil before the parent ion has gained appreciable kinetic energy, the fragment ion formed will pass through the full acceleration potential and will appear as a sharp (prompt) peak. If, however, break-up occurs at a somewhat greater distance from the foil, a fraction of the kinetic energy gained by the parent ion during acceleration to the point of fragmentation will be carried off by the neutral fragment. After passing through the remaining accelerating field, these delayed fragment ions will possess a lower kinetic energy (velocity) than prompt fragment ions. They will thus comprise a high-time tail on the sharp fragment ion peak. The fraction of fragment ions which contribute to the sharp peak will naturally depend on the magnitude of the field in the acceleration region and on the magnitude of the rate constant for the fragmentation reaction. Thus an investigation of the effect of changes in the acceleration field on the shape and magnitude of a fragment ion peak can provide information about the fragmentation process.

Case 2. By a line of reasoning analogous to that outlined above it is appar-

ent that parent ions breaking up just prior to attaining full acceleration will produce a low-time tail on a sharp, undissociated parent ion peak. Disintegrations occurring between these two limits will contribute to a continuum between the fragment ion peak and the parent ion peak.

RESULTS

The tripeptide AlaAlaAla (MW = 231) served as a model system and was examined in detail. The quasi-molecular ion region is shown in Fig. 2(A), where two major species are observed, i.e. the $(M + H)^+$ ion at m/z 232 and the $(M + Na)^+$ ion at m/z 254. These data were recorded with +10 kV on the sample foil, 0 V on the acceleration grids 1 and 2, and 0 V on the deceleration grids B and C (Fig. 1). It is immediately apparent that the peak corresponding to the protonated molecular ion is substantially broader than that of the sodium-cationized species. The former exhibits an FWTM of 3.3 daltons and an FWHM of 0.43 daltons, while the corresponding values for the latter are FWTM = 0.44 daltons and FWHM = 0.13 daltons. The resolution of 1950 (FWHM) observed for the $(M + Na)^+$ peak corresponds approximately to the limiting resolution of the present device at this mass. It should be noted that although the height of the $(M + H)^+$ peak is only 70% that of the $(M + Na)^+$ peak, the integrated intensity of the former ion is 2.4 times that of the latter.

As a hypothesis we assumed that the peak broadening observed was due to metastable decompositions. A series of increasing voltages were applied to the three-element deceleration unit (grids A, B, and C in Fig. 1). As this

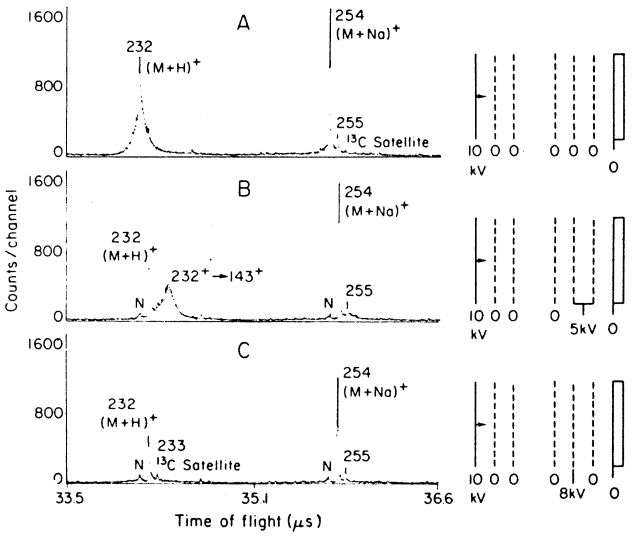

Fig. 2. Quasi-molecular ion peaks in alanylalanylalanine; $(M + H)^+$ and $(M + Na)^+$ peaks at three retarding potentials: A, 0 V; B, 5 kV; and C, 8 kV.

deceleration voltage was increased a broad component of the $(M + H)^+$ peak was observed to shift to longer flight times with respect to a narrow component of the $(M + H)^+$ peak. This is the behavior expected for metastable product ions decomposing in the field-free flight tube and is illustrated in Fig. 2(B) (deceleration potential $V_3 = 5$ kV, i.e. half the acceleration potential). As the deceleration potential is further increased, the metastable-decay product ions move to increasingly higher flight times with respect to the unfragmented parent ions, and they are finally suppressed altogether, as shown in Fig. 2(C), where $V_3 = 8$ kV. Measurement of the metastable ion suppression voltage, i.e. that for which $E_f' = 0$ (eqn. 3), yields the mass of the fragment ion. For AlaAlaAla the ion suppression voltage shows that the bulk (>90%) of the observed metastable decay giving rise to the broadening of $(M + H)^+$ occurs through a single decomposition to a fragment ion with a mass of 143.5 ±1.0 daltons. The probable reaction is

$$(M + H)^+ \rightarrow NH_2CH(CH_3)CONHCH(CH_3)C{\equiv}O^+ + NH_2CH(CH_3)COOH \qquad (5)$$

m/z 232 m/z 143

The AlaAlaAla spectrum contains a normal fragment ion of moderate intensity at m/z 143. In principle the shape of the intensity versus retardation-potential plot at threshold should yield directly the energy spread of the fragment ions. In practice this measurement was not possible in our apparatus since the deceleration assembly produced a considerable apparent energy spread in the retarded ions (~50 V at 5 kV deceleration). The probable origin of this spread is local field inhomogeneities [16] between the grid wires and/or edge effects of the grid electrodes taken as a whole. However, a lower limit for the energy spread can be inferred from the time spread of the separated metastable component (see, for example, Fig. 2(B)). For fragmentations which occur at the beginning of the field-free flight tube, the energy spread ΔE is related approximately to the measured time spread Δt according to

$$\Delta E/E_f = 2\Delta t/t \qquad (6)$$

Since fragmentations may occur along the length of the flight tube, the value of ΔE obtained from eqn. (6) will represent a lower limit. This measurement was made for the metastable transition $232^+ \rightarrow 143^+$ in AlaAlaAla at both 5 and 10 kV acceleration voltages, and the results are shown in Table 1. Also shown are lower limits for T, the internal energy that is converted into translational energy during this fragmentation, obtained using eqn. (4).

Comparison of the peak intensities shown in Fig. 2(A) and (C) yields the fraction of QM ions which either do not fragment in flight or fragment to a daughter ion with a mass >8/10 that of the parent ion. These fractions are 0.18 for $(M + H)^+$ and 0.54 for $(M + Na)^+$. Comparison of these figures also illustrates the resolution improvement obtainable when metastable fragment ions are rejected. The $(M + H)^+$ peak is greatly sharpened, and is now clearly resolved from the ^{13}C satellite peak.

TABLE 1

ΔE measurements for the metastable transition $232^+ \rightarrow 143^+$ in AlaAlaAla

Acceleration potential V_1 (kV)	ΔE (eV)	T (meV)
5	26 ± 5	36 ± 14
10	35 ± 5	32 ± 9

Figure 2(C) also shows small neutral molecular peaks labeled N which are not shifted in time with respect to the unretarded QM ion peaks. The peak intensities are small (5% and 8%, respectively, of the unretarded $(M + H)^+$ and $(M + Na)^+$ intensities) because the long flight tube (3 m) acts as an efficient neutral-particle filter. The presence of the electrostatic particle guide effects efficient collection of ions.

Careful inspection of the sharp residual $(M + H)^+$ peak in Fig. 2(C) reveals a high-time tail. As discussed in the previous Section, such tailing may result from decay during acceleration (close to the sample foil) of a larger parent ion. A search for a high-mass candidate revealed a small $(2M + H)^+$ association ion at m/z 463 with an intensity of 8% relative to the $(M + H)^+$ ion. A plot of this region of the spectrum is shown in Fig. 3(A) for ions accelerated to 10 keV and with 0 V on the repeller. A broad peak (FWTM = 6.0 daltons, FWHM = 2.1 daltons) at m/z 463 is observed, indicating that this ion is decaying in flight. Application of 4.047 kV to the deceleration electrodes resulted in the separation of this broad peak into a sharp component and a broad component (Fig. 3(B)) corresponding to ions which have undergone the reaction

$$(2M + H)^+ \rightarrow (M + H)^+ + M \qquad (7)$$

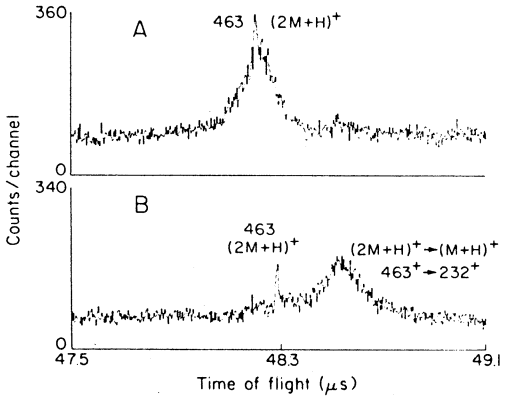

Fig. 3. The $(2M + H)^+$ peak in alanylalanylalanine at two repeller voltages: A, 0 V; B, 4.047 kV.

The measured width of the broad peak indicates a lower limit for T of 36 ± 19 meV.

As discussed in the previous Section, metastable transitions may also be investigated by varying the magnitude of the accelerating field between the sample foil and the first grid. Part of such an investigation is illustrated in Fig. 4(A) and (B), where the acceleration parameters used to obtain these spectra of AlaAlaAla were V_1 = 10 kV, V_2 = 0 V and V_1 = 10 kV, V_2 = 9 kV, respectively. The resultant difference by a factor of 10 in the field strength translates into a difference in the acceleration time to the first grid, t_a, of $\sqrt{10}$, since $t_a \propto [q(V_1 - V_2)]^{-1/2}$. The values of t_a for the m/z 232 parent ion in the two cases are 99 ns and 312 ns. No decelerating field was applied in these cases.

The spectra shown in Fig. 4 were normalized so that the $(M + Na)^+$ peaks had the same height. The mode of representation in Fig. 4 makes the $(M + H)^+$ intensity fortuitously equal to that of $(M + Na)^+$. Several ions in the low-acceleration-field spectrum (Fig. 4(B)) display enhanced peak intensities compared to those of the high-field spectrum, and some remain unchanged. The ions with enhanced intensity are those with m/z 115, 143, and 161. The m/z 84, 99, and 185 ions show little or no change. It has been shown [3] that the most intense ion in the AlaAlaAla spectrum is the fragment ion at m/z 44 ($CH_3CH{=}NH_2^+$) (RI = 50.8% of total ionization), and the intensity of this ion is independent of the value of V_2. Our experiments with retarding potentials showed that the $242^+ \rightarrow 143^+$ decomposition occurred in part as a metastable process in the flight tube. The enhanced m/z 143 intensity observed in Fig. 4(B) indicates that decompositions producing this ion also occur in the first acceleration region. Retarding experiments provide no strong evidence for metastable formation of m/z 115 and 161 ions, and the intensity changes found in the V_2 variation experiments may result from

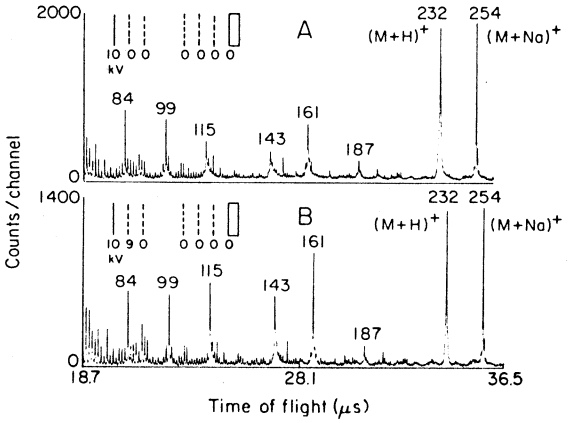

Fig. 4. Alanylalanylalanine spectra (partial) at two first accelerating grid potentials: A, 0 V; B, 9 kV.

relatively large decomposition rate constants and/or the occurrence of further fragmentation of the fragment ions. The m/z 44 ion shows no metastable formation component and also its intensity is independent of the value of V_2. This suggests that the rate constant for the formation of this ion is very large (i.e., fragmentation is complete in a short time), and this suggestion is compatible with the large intensity of the ion. Clearly, these systems which involve the possibility of sequential reactions having various reaction rates are complex and their elucidation will require extensive efforts.

We have not yet made a serious attempt to ascertain quantitatively rate constants for the various fragmentations. It is, however, apparent that the half-lives of the reactions producing ions whose intensities are affected by the value of V_2 are comparable to the acceleration times of the parent ions, i.e. ~100 ns. Probable mechanisms producing the fragments at m/z 115 and 161 are

$$(M + H)^+ \rightarrow NH_2CH(CH_3)\overset{+}{C}ONH{=}CH(CH_3) + HCONHCH(CH_3)COOH \qquad (8)$$

m/z 115

and

$$(M + H)^+ \rightarrow \overset{+}{N}H_3CH(CH_3)CONHCH(CH_3)COOH + NH_2C(CH_3){=}C{=}O \qquad (9)$$

m/z 161

Figure 4A shows that the m/z 115 and 143 peaks in particular display the high-time tailing expected for ions produced by a fragmentation process where the rates are such that detectable amounts of fragmentation occur close to the sample foil. From a calculation involving the magnitude of the acceleration field and the masses of the entities involved, the result is obtained that ions comprising the high-time tail of the m/z 143 ion, for example, are formed 5—30 ns after the passage of the initiating fission fragment. This tailing phenomenon may be useful for obtaining information about fast fragmentation processes in a manner analogous to that already in use in field ionization mass spectrometry [17].

It has been assumed in this work that the observed effects are due to unimolecular dissociation of ions excited during the desorption and ionization process. It is also possible that collision-induced dissociation with residual gas molecules along the extended (3-m) path of the ions in the flight tube might occur. We have carried out experiments to ascertain whether or not this is the case. Figure 5 shows the integrated intensities of the separated sharp and broad components of the $(M + H)^+$ peak and the $(M + Na)^+$ peak of AlaAlaAla as a function of pressure in the flight tube. The acceleration potential for these measurements was 5 kV and the retarding potential 2.8 kV. The pressure was adjusted to values between 5.4×10^{-8} and 2.7×10^{-6} torr, which correspond to a range over a factor of 50. All three peak intensities decrease slightly as the pressure increases, but the effect on the broad and narrow components is the same (bottom plot of Fig. 5). Clearly, collision-

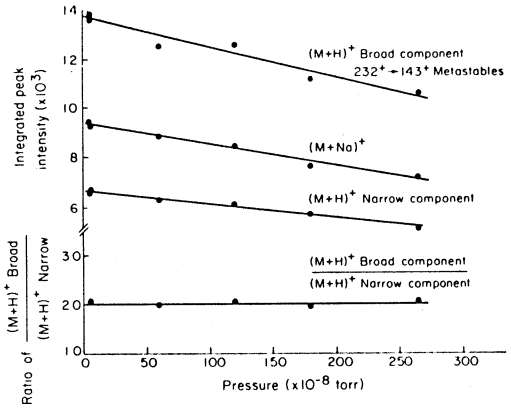

Fig. 5. Alanylalanylalanine QM ion intensities at several pressures.

induced dissociation is not a significant factor in the observed results.

Figure 2 shows that suppression of the metastable fragment ions leads to significant resolution improvements for QM ions from alanylalanylalanine. Several other compounds including guanosine, 5′-AMP, erythromycin, and chlorophyll *a* were investigated and in all cases a useful resolution enhancement was found using this method. Two illustrative examples are given below.

The positive-ion spectrum for guanosine recorded without a retarding field displays (Fig. 6(A)) $(M + H)^+$ and $(M + Na)^+$ QM ion peaks, with both peaks

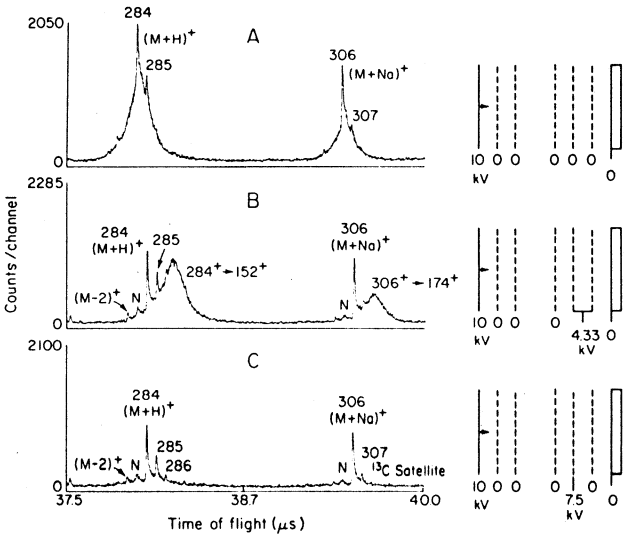

Fig. 6. Quasi-molecular ion peaks in guanosine; $(M + H)^+$ and $(M + Na)^+$ peaks at three retarding potentials: A, 0 V; B, 4.33 kV; and C, 7.5 kV.

considerably broadened. The broadening was determined by the retarding potential method to arise primarily from decays to fragments with m/z 153.0 ±1.0 and m/z 175.2 ±1.0, respectively. Very strong $(\text{base} + 2)^+$ and $(\text{base} + 1 + \text{Na})^+$ fragment peaks are observed at m/z 152 and m/z 174 in the guanosine spectrum [3], and the possible metastable transitions are

$$(\text{M} + \text{H})^+ \rightarrow (\text{base} + 2\ \text{H})^+ + \text{neutral} \qquad (10)$$

m/z 152

$$(\text{M} + \text{Na})^+ \rightarrow (\text{base} + \text{H} + \text{Na})^+ + \text{neutral} \qquad (11)$$

m/z 174

The partially separated sharp and broad components are shown in Fig. 6(B). Lower limits on the kinetic energy release T, deduced from the widths of the broad components, are 63 ±16 meV for reaction (10) and 35 ±12 meV for reaction (11). Figure 6(C) shows the spectrum obtained when a deceleration potential large enough to suppress most of the metastable fragments is applied. The original broad peak splits clearly into four major components one of which (labeled N) corresponds to the unretarded neutral entities. An unusual detail for which no explanation is apparent concerns the large intensity of the m/z 285 peak relative to that of the m/z 284 $(\text{M} + \text{H})^+$ peak. The intensity is 3.2 times that expected for the ^{13}C satellite. We note, in contrast, that the m/z 307 peak has an intensity consistent with that expected for the $(\text{M} + \text{Na})^+$ ^{13}C satellite.

The broad chlorophyll a QM peak (FWTM = 16.0 daltons, FWHM = 6.6 daltons) (Fig. 7(A)) is also observed to split into several discrete components upon application of the decelerating field (Fig. 7(B)). The peak labeled 1 has an experimentally determined mass of 892.581, which corresponds to that

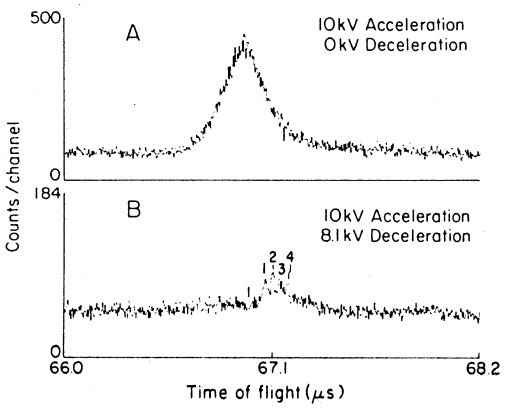

Fig. 7. Quasi-molecular ion peaks in chlorophyll a at two retarding potentials: A, 0 V; B, 8.1 kV.

expected for the $M^{+\cdot}$ ion (892.535) to within 46 m.m.u. The peak labeled 2, with m/z 893.520, has a substantially greater intensity than that expected for the ^{13}C satellite of the $M^{+\cdot}$ ion, and thus is thought to contain a substantial component of $(M + H)^+$. The peaks labeled 3 and 4 were determined to have experimental masses of 894.681 and 895.611, respectively. These are probably ^{13}C satellite peaks, although the intensity relations are not completely appropriate to this hypothesis. We cannot eliminate the possibility that other, unknown phenomena may be operating. It is noteworthy that only 4% of the original unretarded QM ion intensity is retained in these four peaks after fragments with a mass less than $8.1/10.0 \times 892 = 723$ are rejected. The reason for this is that chlorophyll *a* is found to lose its phytol tail and several side-chains on the porphyrin ring readily.

CONCLUSIONS

It has been shown that metastable decomposition of ions during acceleration and in the field-free flight tube are clearly responsible for many of the peak shapes observed in ^{252}Cf time-of-flight mass spectrometry. This phenomenon is expected to be of greater importance for larger molecules which take longer to extract, have longer flight times, and have more decomposition channels. However, time-of-flight mass spectrometry may be the optimal procedure for observing massive short-lived species because the metastable fragments are largely collected and contribute to the parent ion intensity. Practically, QM ion intensity enhancements are expected if the acceleration time can be decreased significantly.

ACKNOWLEDGEMENTS

This work was supported by a grant from the Division of Research Resources, National Institutes of Health. We thank Joseph Shpungin for assistance in the project and Gladys Roberts for secretarial help.

REFERENCES

1 R.D. Macfarlane and D.F. Torgerson, Science, 191 (1976) 920.
2 R.D. Macfarlane, in R. Waller and O.C. Dermer (Eds.), Biochemical Applications of Mass Spectrometry, First Supplementary Volume, Wiley, New York, 1980, Ch. 38.
3 B.T. Chait, W.C. Agosta and F.H. Field, Int. J. Mass Spectrom. Ion Phys., 39 (1981) 339.
4 R.D. Macfarlane, in Trace Organic Analysis: A new Frontier in Analytical Chemistry, Proc. 9th Materials Research Symp., April 1978, Gaithersburg, MD, Natl. Bur. Stand., Spec. Publ. 519, April 1979.
5 C.J. McNeal, S.A. Narang, R.D. Macfarlane, H.M. Hsiung and R. Brousseau, Proc. Natl. Acad. Sci. U.S.A., 77 (1980) 735.
6 J.E. Hunt, R.D. Macfarlane, J.J. Katz and R.C. Dougherty, Proc. Natl. Acad. Sci. U.S.A., 77 (1980) 1745.
7 R.D. Macfarlane and D.F. Torgerson, Int. J. Mass Spectrom. Ion Phys., 21 (1976) 81.

8 W.W. Hunt, R.E. Huffman and K.E. McGee, Rev. Sci. Instrum., 35 (1964) 82.
9 W.W. Hunt, R.E. Huffman, J. Saari, G. Wassel, J.F. Betts, E.H. Paufve, W. Wyess and R.A. Fluegge, Rev. Sci. Instrum., 35 (1964) 88.
10 W.W. Hunt and K.E. McGee, J. Chem. Phys., 41 (1964) 2709.
11 R.E. Ferguson, K.E. McCulloh and H.M. Rosenstock, J. Chem. Phys., 42 (1965) 100.
12 D.L. Dugger and R.W. Kiser, J. Chem. Phys., 47 (1967) 5054.
13 W.J. Haddon and F.W. McLafferty, Anal. Chem., 41 (1969) 31.
14 J.H. Beynon, R.A. Saunders and A.E. Williams, Z. Naturforsch., 20a (1965) 180.
15 R.G. Cooks, J.H. Beynon, R.M. Caprioli and G.R. Lester, Metastable Ions, Elsevier, Amsterdam, 1973.
16 M.Y. Bernard, J. Phys. Radium, 14 (1933) 451.
17 H.D. Beckey, Principles of Field Ionization and Field Desorption Mass Spectrometry, Pergamon, Oxford, 1977, Ch. 4.